A Remedy for Heterogeneous Data: Clustered Federated Learning with Gradient Trajectory

Ruiqi Liu, *Student Member, IEEE*, Junbo Wang, *Member, IEEE,* Songcan Yu *Student Member, IEEE*, Krishna Kant *Fellow, IEEE,*

***Abstract*—Federated Learning (FL) has recently attracted a lot of attention due its ability to train a machine learning model using data from multiple clients without divulging their privacy. However, the training data across clients can be very heterogeneous in terms of quality, amount, occurrences of specific features, etc. In this paper, we demonstrate how the server can observe data heterogeneity by mining gradient trajectories that the clients compute from a two-dimensional mapping of high-dimensional gradients computed by each client from its bottom layer. Based on these ideas, we propose a new Clustered Federated Learning method called CFLGT, which dynamically clusters clients together based on the gradient trajectories. We analyze CFLGT both theoretically and experimentally to show that it overcomes several drawbacks of mainstream Clustered Federated Learning methods and outperforms other baselines.**

***Index Terms*—Federated Learning, Clustering, Heterogeneous Data, Distributed System**

I. Introduction

THe key driver of sophisticated deep learning is the availability of vast amounts of data; however, the data is often produced at many different locations and typically owned by different parties. It is generally not possible to collect all the required data in a central place for deep learning both because of the difficulty of sending and centrally storing the data and because the parties that generate them are unlikely to share it freely [1]. Federated Learning (FL) was proposed to solve this problem [2], where clients in FL keep their data locally. In the typical federated learning framework (FedAvg) [2], the server broadcasts a global model to several clients, and each client trains it with their data and uploads the model to the server. After receiving all updated models, the server aggregates them into a new global model for the next round of training. The server can thus utilize the data owned by different clients for training without the clients having to disclose the data.

But FL still faces a host of challenges. One of them is training with heterogeneous data [3] since the data from different clients could have varying quality, size, features, etc. This can cause several problems in FL, such as bad model performance [4], [5], slow or unstable convergence in training [6], and so on. Several methods have been proposed to reduce the harmful effects from heterogeneous data. References [7]–[9] optimize FL with heterogeneous data via meta-learning, which empowers client model to learn on new data quickly. [10]–[13] propose personalized federated learning, where clients adjust the global model to get a unique model suitable for local data. The contribution of different level layers has also been analyzed recently [12], [14]–[16]. In addition, clustering-based federated learning is implemented to mitigate the negative effects of heterogeneous data. The server collects information from all active clients in FL system and iteratively(or recursively) assigns clients into clusters, where every client in the same cluster has similar data distribution. Thus the non-IID data among all clients can be transformed into IID data in every client cluster. As the input to server for client clustering, the information sent from participating clients effects results of the clustering and update of FL model, which defines the performance of algorithm.

Cluster FL drawbacks with information used: 1) how to estimate the number of clusters, 2) how do we ensure that the data transfer bandwidth between clients and the server is well constrained, 3) how do we ensure that the computing requirements of the client-server coordination are low, and 4) how do we ensure that the additional data exchange does not leak client's data. We managed to extract information from high-level layers in model on client side. Recent research on FL with Non-IID data explicitly or implicitly focus on the high-level layers in FL. They shows that utilizing bottom layer characteristics to enhance FL performance with heterogeneous data is feasible. Thus the research inspired us that we can extract information from high-level layers, send to server and optimize the FL system from an optimal global perspective.

In our work, the gradient information of the bottom layer in client side model is the input of clustered-based Federated Learning. We call it as gradient trajectory, an innovative two-dimensional vector based on gradient decomposition. The gradient trajectory contains client data distribution information with no privacy concern and huge computation cost. Thus the server can achieve accurate client clustering efficiently. Specifically, focused on a classification task with softmax layer and cross entropy loss function, inspired by [15], we decompose the bottom layer gradient into two vectors, pulling force and pushing force. We show that the pulling forces and pushing forces are directly related to dataset distribution. Then we extract distribution information in these two forces to get gradient trajectory of clients. The trajectories are composed of points connected in two dimensions, produced by two forces. [15]. And with clients' privacy guaranteed, we explain why the

Ruiqi Liu, Junbo Wang and Songcan Yu are with School of Intelligent Systems Engineering, Sun Yat-Sen University, China.
E-mail: ruiqiliusysu@gmail.com;wangjb33@mail.sysu.edu.cn
Ruiqi Liu is also with College of Engineering, Georgia Institute of Technology, Atlanta, GA, USA.
Krishna Kant is with Computer and Information Science, Temple University, Philadelphia, USA, Email: kkant@temple.edu
Corresponding author: Junbo Wang

server can mitigate heterogeneity in the system with gradient trajectories.

We thus propose a novel Clustered Federated Learning framework called Clustered Federated Learning with Gradient Trajectory (CFLGT) to solve the heterogeneous data problem in FL, which clusters clients accurately and swiftly. Our main contribution can be summarized as follow: 1) We deep dive into the underlying gradients and present the first gradient trajectory for representing data heterogeneity. 2) We theoretically prove the mathematical meaning of the gradient trajectory and explore its potential as a clustering object. 3Based on the study of gradient trajectories, we propose the new FL algorithm and following experiments show that our method mitigates the negative effects of the above drawbacks and achieves excellent performance with a small cost, and is practical in real-world tasks.

II. Related Work

A. FL with heterogeneous Data

Researchers have proposed several methods to handle the heterogeneity problem in FL. Li et al. proposed the FedProx [17], which adds a regularization term to the loss function to prevent the locally trained model from deviating too much from the global model. The studies in [7]–[9] optimize the performance of FL with heterogeneous data by leveraging the fast learning properties of meta-learning for new tasks. Researches in [10]–[12] proposed personalized federated learning to optimize the performance of federated learning by training personalized models for different users. Also several researches have recently investigated the impacts from high-level layers on FL with heterogeneous data. Sun et al. [12] shows that aggregating too many high-level layers will hurt FL performance with heterogeneous data. The experiments in [14] exhibit that the highest disparity occurs between bottom layers of neural networks in FL with heterogeneous data. Li [15] accounts for the influence on the bottom layer in a label-shift condition while clients in FedRep [16] train and keep their high-level layers locally, thus protecting their model from the pollution of heterogeneous data. These works show that high-level layers of a neural network are more sensitive to heterogeneous data in FL than other layers and affects greater model performance because of the closer contact with common features [18].

B. Clustered Federated Learning

Clustered Federated Learning (CFL) [19] techniques can control the aggregation of clients' model by clustering clients into groups. However, the existing works still face quite a few problems.

1) **Data privacy issue**: In the CFL algorithms [19]–[21], clients need to upload the gradient or model to the server. If attackers capture the information, they can complete an inference attack. Zhu et al. [22] demonstrate the possibility of obtaining raw data by intercepting the uploaded gradients and successfully implementing the data-privacy-level attack. In addition, Melis et al. [23] proposes an attack on client's data privacy by obtaining the model update. This attribute inference attack uses the updated model to infer sensitive attributes of the training data. As a result, uploading a model or gradient for clustering is dangerous to clients in the FL system.
2) **The number of cluster needs to be determined in advance**: The popular clustered federated learning algorithms need the number of clusters in advance as the algorithm's input. However, it is difficult to determine a reasonable number of clusters on the server-side in a real scenario, considering the huge scale of participating clients and data privacy constraints. Additionally, a wrong cluster number may damage the FL performance, which is shown in our experiments.
3) **Ignoring the limitation of bandwidth and client's computing power**: When the number of clusters is large and the model structure is complex, IFCA [24] needs to broadcast all clusters' global models to clients in each round, which requires considerable pressure on the bandwidth and user's computing resources. Moreover, Gholizadeh et al. [25] proposes an algorithm that uses model hyper-parameters for clustering. The user uses grid search to find the optimal hyper-parameters (including the number of neurons and epochs) and uploads them to the server-side. When using large models, grid search will consume computational resources greatly, even exceeding the client's limitation.

III. Formulation of Gradient Trajectory

In this section, we show how a server explores the bottom layer's gradient information. First, we introduce basic concepts of Federated Learning (FL) and properties of the bottom layer with softmax (classifier). Then we transform the gradient into gradient trajectories in subsection 3.2. Thus, the server can receive the trajectories from clients with privacy guarantees and observe the data heterogeneity in the FL system by mining trajectories simultaneously.

A. Basic concepts

Basic Concepts of Federated Learning: In a typical FL system with a classification task, there is one machine learning agent in the "server" and M machine learning agents in clients. The server broadcasts global model h_0 to the participating clients and receives clients' model $h_m (m \in [1, M])$ from the clients in each round. Each client owns a dataset D_m containing N_m samples for local training, denoted as $(\boldsymbol{x}_{m,i}, y_{m,i})_{i=1}^{N_m}$, where i indicates a sample in D_m. In the t-th round of learning, the server randomly select a subset of clients U^t among M clients and broadcasts the current global model h_g^{t-1} to them. Once receiving the h_g^{t-1}, each client m in U^t updates it by performing local training with data D_m with the objective:

$$\min_{h_m^t} \mathbb{E}_{(\boldsymbol{x},y)\sim D_m} \left[F\left(h; \boldsymbol{x}, y\right)\right], \tag{1}$$

where F indicates the loss function. After local training, the client uploads its new model h_m^t to the server. When all models are received, the server aggregates them together as a new global model h_g^t as follows,

$$h_g^t = \frac{1}{\sum_{m\epsilon U^t} |D_m|} \sum_{(m\epsilon U^t)} |D_m| \, h_m^t. \tag{2}$$

Properties of Softmax Layer: Like [14], [15], we decompose a neural network into a feature extractor and classifier. The classifier represents the bottom layers with weights in a network, and the rest of the layers are feature extractors. After the i-th sample enters the neural network, the feature extractor outputs the extracted feature vector, denoted as $\boldsymbol{v}_i \in \mathbb{R}^d$. For a C-classes classification task, the weights in the classifier can be written as $\boldsymbol{W} = \{\boldsymbol{w}_c\}_{c=1}^C \in \mathbb{R}^{d\times C}$ (the bias in the classifier is omitted). Then the classifier receives the $\boldsymbol{v}_i$ and outputs the probability vector of the i-th sample by $\boldsymbol{P} = \text{Softmax}(\boldsymbol{W}^T\boldsymbol{v}_i)$. Specifically, the probability that the i-th sample belongs to class c-th class can be written as:

$$P_{i,c} = \frac{exp(\boldsymbol{w}_c^T\boldsymbol{v}_i)}{\sum_{j=1}^C exp(\boldsymbol{w}_j^T\boldsymbol{v}_i)}. \tag{3}$$

As cross-entropy loss is implemented and denoted as

$$\mathcal{L} = \sum_{i=1}^N \sum_{c=1}^C \mathcal{I}\{y_i = c\}\log(P_{i,c}), \tag{4}$$

where $\mathcal{I}\{\cdot\}$ is the indicator function. The gradient of c-th weights is calculated as

$$\boldsymbol{g}_{\boldsymbol{w}_c} = -\sum_{i=1}^N (\mathcal{I}\{y_i = c\} - P_{i,c})\boldsymbol{v}_i, \tag{5}$$

which equals to

$$\boldsymbol{g}_{\boldsymbol{w}_c} = -\sum_{i=1, y_i = c}^N (1 - P_{i,c})\boldsymbol{v}_i + \sum_{i=1, y_i \neq c}^N (P_{i,c})\boldsymbol{v}_i. \tag{6}$$

Borrowing from previous works [15], [26]–[28], we call the first term as pulling force $\boldsymbol{Z}_1$, consisting of extracted feature from positive samples ($y_i = c$). For the second term, which consists of extracted features from negative samples ($y_i \neq c$), we call it pushing force $\boldsymbol{Z}_2$. An example of this decomposition is shown in Figure 1. In summary, the gradient of the softmax layer can be divided into pulling force and pushing force, which has a practical meaning in mathematics.

B. From Gradient to Trajectory

In a FL system with heterogeneous data, obtaining the distribution of clients' datasets is beneficial to optimize the FL system. However, uploading class statistic of client dataset may cause user-level label leakage [29], thus it is not wise for client to send dataset statistic to server. Thanks to the mechanism of FL, every client who receives the same global model in each round can compute its pulling force and pushing force by Eq. (6) on local data and then upload them. In this way, the server can be aware of the system's heterogeneity by analyzing the values of pulling force and pushing force.

Yet the strategy poses a huge risk of a data privacy breach. Note that an attacker can restore the gradient of the bottom layer by simply combining pulling force with pushing force. As a result, attack to data privacy in [30], [31] can be implemented by capturing pulling force and pushing force.

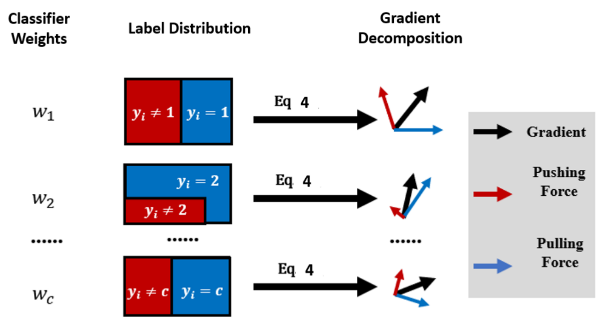

Fig. 1. Classifier Weights Gradient Composition. In a c-th classes classification task, the gradient of each weight in the classifier can be divided into pulling force and pushing force by data labeled as c and labeled not as c.

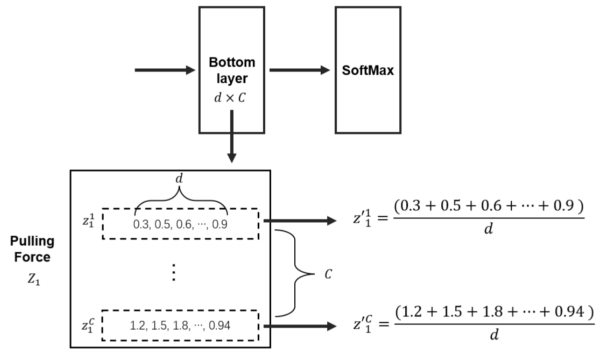

Fig. 2. The computation of Z'^j_i. The figure shows a toy example of Z'^j_1 formation. The bottom layer is shaped as $d \times C$, thus pushing force $\boldsymbol{Z}_1$ has the same shape. $\boldsymbol{Z}_1$ has C vectors as z_i^j, which contains d values. For every z_i^j, we average it to get Z'^j_i.

Therefore, we propose a method to transform pulling force and pushing force into gradient trajectory, uploaded to a server with privacy protected. Gradient trajectory is a computed projection of pulling force and pushing force into a two-dimensional space.

To be specific, after receiving the global model, client computes pushing forces $\boldsymbol{Z}_1$ and pulling forces $\boldsymbol{Z}_2$ by Eq. (6)

$$\boldsymbol{Z} = (\boldsymbol{Z}_1, \boldsymbol{Z}_2) = \left(\left[z_1^1, z_1^2, \cdots, z_1^C\right], \left[z_2^1, z_2^2, \cdots, z_2^C\right]\right), \tag{7}$$

where C represents the number of classes in the task, and $[\boldsymbol{z}_i^j], i \in [1,2], j \in [1, \cdots, C]$ is a vector shaped as $[d, 1]$, where d is the shape of classifier input (also is the output of feature extractor). Then we compute $[\boldsymbol{Z}'^j_i], i \in [1,2], j \in [1, \cdots, C]$, by averaging all the values in corresponding vector $\boldsymbol{z}_i^j$. Figure 2 displays an example. With this method, we average every vector in $\boldsymbol{Z}_1$ and $\boldsymbol{Z}_2$ and then transform them to $\boldsymbol{Z}'_1$ and $\boldsymbol{Z}'_2$ as follow:

$$\begin{aligned} \boldsymbol{Z}'_1 &= \left[Z'^1_1, Z'^2_1, \cdots, Z'^C_1\right]^T = \left[avg(z_1^1), \cdots, avg(z_1^C)\right]^T, \\ \boldsymbol{Z}'_2 &= \left[Z'^1_2, Z'^2_2, \cdots, Z'^C_2\right]^T = \left[avg(z_2^1), \cdots, avg(z_2^C)\right]^T. \end{aligned} \tag{8}$$

Because of the above transformation, $\boldsymbol{Z}'_1$ and $\boldsymbol{Z}'_2$ inherit mathematical meaning from $\boldsymbol{Z}_1$ and $\boldsymbol{Z}_2$, that is the norm of

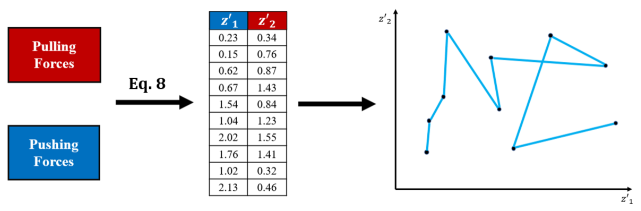

z'_1	z'_2
0.23	0.34
0.15	0.76
0.62	0.87
0.67	1.43
1.54	0.84
1.04	1.23
2.02	1.55
1.76	1.41
1.02	0.32
2.13	0.46

Fig. 3. The formation of gradient trajectory. In a 10-th classes classification task, a client calculates its pulling force and pushing force, gets $\boldsymbol{Z}'_1$ and $\boldsymbol{Z}'_2$, and plots the trajectory in a two-dimensional space, where x axis is for $\boldsymbol{Z}'_1$ and y axis is for $\boldsymbol{Z}'_2$.

these two high dimensional vectors. Note that $[z_i^j] \geq 0$ because $P_{i,k}, (1 - P_{i,k}) \geq 0$ and $\boldsymbol{v}_i$ is the output of activations(e.g. sigmoid, relu), which cannot be negative value. Therefore, $[Z_i'^j]$ equal to ratio between L1 norm of $[z_i^j]$ and their size. Because the size is constant, decided by the model in FL system. We can see that $\boldsymbol{Z}'_1$ and $\boldsymbol{Z}'_2$ composed of $[Z_i'^j]$, are considered as the deformation of L1 paradigm, which represents the values of $\boldsymbol{Z}_1$ and $\boldsymbol{Z}_2$. In this way, our transform method passes the mathematical significance of pulling force and pushing force to $\boldsymbol{Z}'_1$ and $\boldsymbol{Z}'_2$.

To form the gradient trajectory, a client puts $\boldsymbol{Z}'_1$ and $\boldsymbol{Z}'_2$ into the two-dimensional space, gets C points, and then gets its gradient trajectory by connecting C points in a certain order, which given by the server. The order is randomly computed by server and applied to all clients' $\boldsymbol{Z}'_1$ and $\boldsymbol{Z}'_2$ for trajectory visualization. Figure 3 displays a gradient trajectory of a client in the FL system.

C. Data Heterogeneity Observation by Gradient Trajectory

In this part, we set up a FL system based on FedAvg [1] to illustrate the analysis of data heterogeneity with gradient trajectories from clients. During training rounds, all clients in the system receive a new global model, compute pulling force and pushing force, and upload their own gradient trajectories. From server's perspective, the data heterogeneity in FL system has became gradient trajectories from all clients. To gain a deep insight into data heterogeneity, the server can observe the gradient trajectories by qualitative and quantitative analysis. For better comparison, we set up two data distributions in the system, IID data and heterogeneous data.

Qualitative Analysis: The server collects all gradient trajectories and visualizes them to observe data heterogeneity. As the left chart in Figure 4 shows, all trajectories in the system with IID data have the same shape, meaning that data distribution across clients is the same too. In the right chart, there are clear distinctions between many trajectories. The trajectories in the red circle have a clear difference from trajectories in the green square, reflecting the diversity across the clients' dataset. Therefore, the trajectory visualization provides a clear picture of the degree of heterogeneity for the server.

Quantitative analysis: In addition to observing heterogeneity at the visualization level, the server also needs specific values to evaluate data heterogeneity. Here server computes

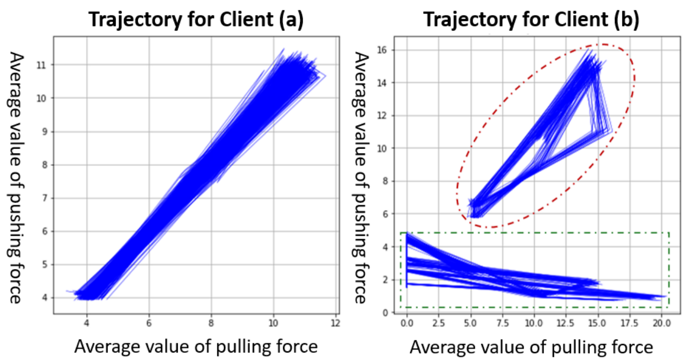

Fig. 4. Gradient Trajectories of all Clients in a FL System. The trajectories in (a) is from IID data and trajectories in (b) is from heterogeneous data.

the coefficient of variation c_v [32] of $\boldsymbol{Z}'_1$ and $\boldsymbol{Z}'_2$ to evaluate heterogeneity in a FL system. The c_v is defined as the ratio of the standard deviation σ to the mean μ. The larger it is, the deviation of data is. It shows that for trajectories in Figure 4 (a), the c_v of x axis and y axis are 0.407 and 0.408. For trajectories in Figure 4 (b), the c_v of x axis and y axis are 0.881 and 1.397. The result implies that the coordinates in the right plot in Figure 4 are more discrete and the points of the trajectory are more sparsely distributed. Therefore, c_v could assist the server in the FL system in calculating the degree of heterogeneity in the FL system.

IV. OUR METHOD

A. Motivation

Though the server can observe heterogeneity with gradient trajectories, it still needs a method that utilizes the information in gradient trajectories to optimize the FL system. Suppose that a server in a FL system with label distribution shift [33] knows roughly the dataset distribution among clients, so it can aggregate clients with similar dataset distribution to improve FL performance. Clustered Federated Learning [19] is an ideal framework where the server clusters clients into groups and executes model aggregation in every cluster. It is possible for servers who obtain all clients' gradient trajectories to cluster clients accurately in the FL system, as the gradient trajectory contains important information, which is illustrated in subsection 4.3.

B. Cluster clients in FL

We introduce our method, Clustered Federated Learning by Gradient Trajectory (CFLGT), where the server collects gradient trajectories of all clients and clusters them into groups, so each group can have its global model achieving a better performance. The algorithm is presented in Algorithm 1. The algorithm firstly runs for K rounds of FedAvg as pre-training. After finishing pre-training, the server broadcasts the current global model h_g to every client in the FL system. Once receiving h_g, client calculates the pulling force $\boldsymbol{Z}_1$ and pushing force $\boldsymbol{Z}_2$ on local data by Eq. (6) and then gets average values of pulling force and pushing force separately $\boldsymbol{Z}'_1, \boldsymbol{Z}'_2$ by Eq. (8). Note that $\boldsymbol{Z}'_1, \boldsymbol{Z}'_2$ are the x- and y-axis coordinates of

Algorithm 1 CFLGT

```
Require: learning rate $\eta$, initial model $h$, set of clients $M$, pre-training rounds $K$, FL rounds $T$, local training epoch $r$.
1: Server: $h_g \leftarrow h$
2: for $t = 0, 1, 2, ..., K-1$ do
3:     $h_g \leftarrow FedAvg(h_g, M)$
4: end for
5: for $m \in M$ in parallel do
6:     get ${}^m\boldsymbol{Z}_1$, ${}^m\boldsymbol{Z}_2$ by Eq. (6)
7:     get ${}^m\boldsymbol{Z}'_1$, ${}^m\boldsymbol{Z}'_2$ by Eq. (8)
8:     send ${}^m\boldsymbol{Z}'_1$, ${}^m\boldsymbol{Z}'_2$ to server
9: end for
10: In server:
11: $C, [h_{g,c}]_{c=1}^{C} \leftarrow AffinityPropagation([{}^i\boldsymbol{Z}'_1, {}^i\boldsymbol{Z}'_2]_{i=1}^{M})$
12: for $t = 0, 1, 2, ..., T-1$ do
13:     $U^t \leftarrow$ random subset of clients $M$
14:     for $\bar{c} \in C$ do
15:         for $client - c \in U^t$ in parallel do
16:             if $clientc \in \bar{c}$ then
17:                 $h_c \leftarrow h_{g,\bar{c}}$
18:                 $h_c \leftarrow$ LocalUpdate($h_c$)
19:                 client sends $\boldsymbol{h}_c$ to server
20:             end if
21:         end for
22:         $\boldsymbol{h}_{g,\bar{c}} \leftarrow \frac{1}{\sum_{m \in U^t \& m \in \bar{c}} N_m} \sum_{(m \in U^t \& m \in \bar{c})} h_{\bar{c},m}$.
23:     end for
24: end for
25: return $[h_{g,\bar{c}}]_{\bar{c}=1}^{C}$
26:
27: LocalUpdate($h_c, r, \eta$) for $m$-th client
28: for $q = 0, ..., r-1$ do
29:     gradient descent $h'_{c,m} = h_{c,m} - \eta \hat{\nabla} F(h_{c,m}, D_m)$
30: end for
31: return $h'_{c,m}$
```

gradient trajectory in the two- dimensional space. $\boldsymbol{Z}'_1, \boldsymbol{Z}'_2$ of every client will be uploaded to the server, which uses gradient trajectories ($\boldsymbol{Z}'_1, \boldsymbol{Z}'_2$ of clients) as input of Affinity Propagation to cluster clients into groups. Specifically, the input of Affinity Propagation is the distance between two trajectories, calculated by averaging L2 distance between corresponding points, such as $(Z_1'^C, Z_2'^C)$ of two trajectories.

Once client clusters defined, the algorithm runs T rounds of Clustered Federated Learning. In each round, the server randomly selects a subset of clients U^t. The client m chooses its group's model $h_{g,\bar{c}}$ as initialization, updates it to $h^m_{c,\bar{c}}$ where c is short for client, and sends it to the server. The server aggregates clients in the same group to update a new $h_{g,\bar{c}}$ for the next round of training.

C. Information in Gradient Trajectory

Why is gradient trajectory the key in our method? The answer lies inside the information in gradient trajectory. Since the gradient trajectory represents the pulling force $\boldsymbol{Z}_1$ and pushing force $\boldsymbol{Z}_2$, and then figuring out what information the $\boldsymbol{Z}_1$ and $\boldsymbol{Z}_1$ carry can help us understand the information gradient trajectory carries.

Information of dataset: According to Eq. (6), it is clear that the value of $\boldsymbol{Z}_1$ and $\boldsymbol{Z}_2$ is directly correlated to the label distribution of the dataset. As a result, reconstructed by $\boldsymbol{Z}_1$ and $\boldsymbol{Z}_2$, the gradient trajectory also has information of dataset distribution.

Information of model update: In this part, we theoretically prove that the gradient norm is greatly effected by $\boldsymbol{Z}_1$ and $\boldsymbol{Z}_2$. According to [34], the $L2$ norm of gradient in l-th layer for i-th sample $(\boldsymbol{x}_i, y_i)$ can be written as:

$$\|\nabla_{\boldsymbol{w}_l} F(h; \boldsymbol{x}_i, y_i)\|_2 \leq \rho \left\| \varpi' diag((\boldsymbol{w}_1^T \boldsymbol{v}_i), \cdots, (\boldsymbol{w}_C^T \boldsymbol{v}_i)) \nabla_{\boldsymbol{P}_i} F \right\|_2, \tag{9}$$

where F is loss function, h is model, ϖ is the softmax function, $\{\boldsymbol{w}_j\}_{j=1}^{C}$ is the weights of bottom layer (classifier), C is the classes of task, $\boldsymbol{v}_i$ is the output of feature extractor of i-th sample, ρ is the coefficient determined by model structure, and $\boldsymbol{P}_i$ is the probability vector of i-th sample (the output of softmax layer).

Since the loss function of i-th sample$(\boldsymbol{x}_i, y_i)$ is represented as

$$F = -\sum_{j=1}^{C} y_{i,j} log P_{i,j}, \tag{10}$$

where $y_{i,j} \in \{0, 1\}$ and $P_{i,j}$ is a non-zero probability value, we can get

$$\|\nabla F(h; \boldsymbol{x}_i, y_i)\|_2 \leq \rho \left\| \varpi' diag((\boldsymbol{w}_1^T \boldsymbol{v}_i), \cdots, (\boldsymbol{w}_C^T \boldsymbol{v}_i))(-\frac{\lg e}{P_{i,k}}) \right\|_2. \tag{11}$$

Note that k is the only class satisfying $y_{i,k} = 1$. The right term of Eq. (11) can be written as

$$\begin{aligned} &\rho^0 \left\| diag(\frac{1}{P_{i,k}} \varpi'(\boldsymbol{w}_1^T \boldsymbol{v}_i), \cdots, \frac{1}{P_{i,k}} \varpi'(\boldsymbol{w}_C^T \boldsymbol{v}_i)) \right\|_2 \\ &= \rho^0 \left\| diag(\beta_1^1, \cdots, \beta_k^2, \cdots, \beta_C^1) \right\|_2. \end{aligned} \tag{12}$$

For $\beta_j^1 (j \neq k)$, we get

$$\begin{aligned} \beta^1 &= \frac{1}{P_{i,k}(\sum_j^C \exp(\boldsymbol{w}_j^T \boldsymbol{v}_i))} \frac{\exp(\boldsymbol{w}_j^T \boldsymbol{v}_i) \exp(\boldsymbol{w}_j^T \boldsymbol{v}_i)}{\sum_j^C \exp(\boldsymbol{w}_j^T \boldsymbol{v}_i)} \\ &= -\frac{1}{P_{i,k}(\sum_j^C \exp(\boldsymbol{w}_j^T \boldsymbol{v}_i))} \sigma_0 \\ &\leq -\frac{\sigma_0}{\sum_j^C [P_{i,k}(1 + (\boldsymbol{w}_j^T \boldsymbol{v}_i))]} \\ &\leq -\frac{\sigma_0}{\sum_j^C [P_{i,k} + (\boldsymbol{w}_j^T P_{i,k} \boldsymbol{v}_i))]}. \end{aligned} \tag{13}$$

Recall that the pulling force $\boldsymbol{Z}_{1,i}$ of a sample can be represented as $P_{i,k} \boldsymbol{v}_i$, so we get

$$\beta^1 \leq B^1 = -\frac{\sigma}{\sum_j^C [P_{i,k} + (\boldsymbol{w}_j^T \boldsymbol{Z}_{1,i}))]}. \tag{14}$$

For $\beta_j^2 (j = k)$, we get

$$\begin{aligned}\beta^2 &= \frac{exp(\boldsymbol{w}_j^T \boldsymbol{v}_i)(\sum_j^C exp(\boldsymbol{w}_j^T \boldsymbol{v}_i) - exp(\boldsymbol{w}_j^T \boldsymbol{v}_i))}{\sum_j^C exp(\boldsymbol{w}_j^T \boldsymbol{v}_i) P_{i,k} \sum_j^C exp(\boldsymbol{w}_j^T \boldsymbol{v}_i)} \\ &= \sigma_1 \frac{1}{P_{i,k} \sum_j^C exp(\boldsymbol{w}_j^T \boldsymbol{v}_i)} \\ &\leq \sigma_1 \frac{1}{P_{i,k} \sum_j^C exp(\boldsymbol{w}_j^T \boldsymbol{v}_i) - \sum_j \boldsymbol{w}_j^T \boldsymbol{v}_i} \\ &\leq \sigma_1 \frac{1}{P_{i,k} \sum_j^C [1 + (\boldsymbol{w}_j^T \boldsymbol{v}_i)] - \sum_j \boldsymbol{w}_j^T \boldsymbol{v}_i} \\ &\leq \frac{\sigma_1}{\sum_j [P_{i,k} - (1 - P_{i,k}) \boldsymbol{w}_j^T \boldsymbol{v}_i]}.\end{aligned} \tag{15}$$

Recall that the pushing force $\mathbf{Z}_{2,i}$ of a sample can be represented as $(1 - P_{i,k})\boldsymbol{v}_i$, so we get

$$\beta^2 \leq B^2 = \frac{\sigma_1}{\sum_j [P_{i,k} - \boldsymbol{w}_j^T \mathbf{Z}_{2,i}]}$$

As a result, the L2 norm of gradient in l-th layer for i-th sample $(\boldsymbol{x}_i, y_i)$ can be written as:

$$\begin{aligned}&\|\nabla_{\boldsymbol{w}_l} F(h; x_i, y_i)\|_2 \\ &\leq \rho^0 \left\| diag(\beta_1^1, ..., \beta_k^2, ..., \beta_C^1) \right\|_2 \\ &\leq \rho^0 \left\| diag(B_1^1, ..., B_k^2, ..., B_C^1) \right\|_2 .\end{aligned} \tag{16}$$

As shown in [35], the $L2$ norm of the gradient reflects the model update characteristics well. The larger the gradient norm, the bigger the contribution to model update of the sample. The Eq. (16) shows that pulling force $\mathbf{Z}_1$ and pushing force $\mathbf{Z}_2$ affect the variation of gradient norm; thus, we can show that $\mathbf{Z}_1$ and $\mathbf{Z}_2$ can show vital information of model update.

In summary, since the pulling and pushing forces carry information of model update and dataset distribution, the gradient trajectory is a good choice for client clustering. In a FL system, a trajectory representing the dataset and model update of the correspondent client. By clustering the trajectories, we can group clients who are similar at the model update and dataset level into the same category, thus alleviating the impact of heterogeneous data.

D. Analysis of CFLGT

Firstly, the point order of trajectory cannot influence the result of client clustering. Though it is the points order that defines the shape of trajectory, our clustering input is a distance matrix, computed by distance between corresponding points of trajectory. Thus, whatever the order is, the distance matrix is fixed and so is the clustering result.

For clients, calculating pulling force $\mathbf{Z}_1$ and pushing force $\mathbf{Z}_2$ does not consume much time. As defined in Eq. (6), the output of feature extractor v and the probability of correct label p are all $\mathbf{Z}_1$ or $\mathbf{Z}_2$ need, which can be obtained in forward propagation. It means a client only needs to complete forward propagation to get its $\mathbf{Z}_1$ and $\mathbf{Z}_2$. Considering that [34] proves that the backward propagation requires about twice the amount of time as the forward propagation since it needs to compute full gradients, calculating $\mathbf{Z}_1$ and $\mathbf{Z}_2$ is not a time-consuming task for a client.

The Affinity Propagation algorithm [36] helps achieve clients to be clustered without a pre-defined number. The success of Affinity Propagation is the apparent clustering trend in the gradient trajectory, which carries client information (proved in the section above). After rounds of pre-training, the gradient trajectories of clients often exhibit great potential for clustering and distinctly different distributions (An example is shown in Figure 5). Besides, we introduce a concept named Hopkins Statistic H [37] to assess the clustering trend of the data. If the data points are uniformly distributed in the space, H is approximately 0.5. If the clustering situation exists in the data set, H will be close to 1. The case that H is higher than 0.75 indicates a clustering trend in the data set at a 90% confidence level. The H of gradient trajectories are usually higher than 0.75, reflecting the clustering trend. As a result, the clustering trend of gradient trajectories ensures that the server can utilize gradient trajectories for client clustering by Affinity Propagation.

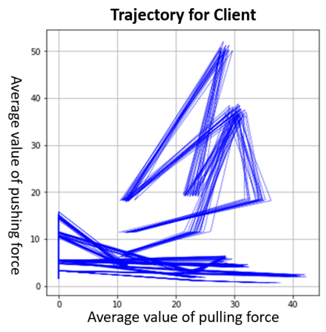

Fig. 5. Gradient Trajectories of 100 clients in a FL System. The trajectories of the 100 clients form several distributions, showing a clear trend of clustering.

One of the concerns about privacy in FL is unintentional data leakage & reconstruction through inference [38], [39], that attackers may obtain the information uploaded by clients to the server and then utilize the information to reconstruct or attack raw data in clients. For privacy protection, our method only requires the client to upload its average values of pulling force $\mathbf{Z}_1'$ and pushing force $\mathbf{Z}_2'$, rather than $\mathbf{Z}_1$ and $\mathbf{Z}_2$. In this way, even though an attacker successfully captures the $\mathbf{Z}_1'$ and $\mathbf{Z}_2'$, it still cannot restore the clients' raw data by the attacking method in [31]. The details in the privacy protection of our method are shown in Section 5.

V. EXPERIMENTS

This section presents the experiments we have performed to evaluate CFLGT. First, we compare CFLGT with other baselines on three scenarios, where heterogeneity is different. Secondly, we experimentally show that CFLGT does not need the number of clusters as input while other Clustered Federated Learning (CFL) methods may suffer from a wrong pre-defined number of clusters. Then a comparative experiment demonstrates that our method is more efficient and can be implemented without significant communication or

TABLE I
PERFORMANCE COMPARISONS WITH OTHER BASELINES ON THREE SCENARIOS.
THE AVERAGE ACCURACY OF THE LAST 20 ROUNDS ARE REPORTED. THE μ IN FEDPROX IS 0.001 [15].

Methods	**Cifar**			**Fmnist**			**SVHN**		
	scenario1	**scenario2**	**scenario3**	**scenario1**	**scenario2**	**scenario3**	**scenario1**	**scenario2**	**scenario3**
Fedavg	46.44%	50.51%	36.23%	79.09%	83.21%	74.45%	25.23%	75.94%	69.89%
Fedavg+FT	78.05%	64.87%	69.03%	97.58%	90.45%	91.14%	57.28%	82.53%	71.07%
Fedprox	40.64%	48.57%	32.02%	78.45%	83.04%	74.72%	25.23%	71.69%	56.86%
Fedsem	73.97%	64.49%	69.10%	99.63%	91.37%	84.86%	74.47%	81.54%	81.12%
FL+HC	81.40%	65.37%	72.70%	99.61%	**92.37%**	84.58%	91.36%	84.69%	85.74%
IFCA	72.80%	60.20%	54.66%	98.87%	91.01%	84.89%	51.03%	80.84%	30.47%
CFLGT	**83.17%**	**65.72%**	**73.49%**	**99.64%**	92.34%	**93.09%**	**92.61%**	**84.91%**	**86.33%**

computation expense. Finally, we show why our method can protect data privacy in clients.

A. Performance Comparison

Experimental Setting: We design three scenarios in experiments, which are done in related works. [19], [40], [41] In the first heterogeneous scenario (scenario 1), we consider that each dataset consists of two types of labels. Take Cifar10 as an example. One dataset can have labels 0 and 1, whereas the other has labels 1 and 3. We form five types of label combinations randomly from these to indicate different data distributions. After that, each client randomly chooses one label combination and is assigned 50 samples for each type of label. Note that the selected sample will not be selected again. As a result, the FL system finally has 100 clients with 50×2 training samples in one client. Since clusters should be generated based on types of data distribution, the clients can naturally form 5 clusters.

The second heterogeneous scenario (scenario 2) is similar to the first one, except that we consider five labels in each combination, so a client in the second scenario has 50×5 training samples in one client.

The third heterogeneous scenario (scenario 3) also follows scenario 1, but there are twenty combinations in all, and every combination contains three types of labels. Considering that every client selects one from 20 twenty combinations and the server does not exactly know the combination of every client, it is possible that FL system contains less than 20 data distributions, making scenario 3 a more challenging task. For other CFL methods, we suppose that the clients form twenty clusters based on the data distribution, and the FL system in scenario 3 has 100 clients with 50×3 samples in a client.

The three scenarios are implemented with Cifar10, FashionMNIST, and SVHN. Lenet (A CNN in Python) is chosen in Cifar10 and Street View House Numbers (SVHN) Dataset and a 2-layers DNN is for FashionMNIST. We take 200 global rounds (100 global rounds in FashionMNIST) and extra 25 pre-training rounds for Clustered Federated Learning baselines with a batch size of 32, SGD with momentum 0.9 as the optimizer, and a learning rate 0.001. In each training round, 20% clients are chosen to participate in training, and accuracy is calculated by averaging accuracy on the test dataset across all clients.

Baselines: We compare CFGLT with other CFL algorithms, including FL+HC based on model parameters, FedSem based on model L2-distance, and IFCA based on models' local performance. In FL+HC, the server receives the update of the client model and uses Hierarchical Clustering [42] to assign clients into groups. In Fedsem, after obtaining updated models from clients, the server assigns the client into the corresponding group with L2-distance of models. In IFCA, the server only stores global models of all clusters while every client chooses its group based on the global models' performance on the local dataset. Some popular FL algorithms are also involved: FedAvg, FedProx based on regularization in the loss function, and FedAvg+FT, where after receiving the global model, the client will update the bottom layer of the model on its data. FedAvg+FT is proved as a powerful and straightforward Personalized Federated Learning method in [16].

For a fair comparison, all clustering methods are completed in the pre-training round, where all clients are involved. After entering the global training, each client will not be moved to another group. This setting can help us know the efficiency and accuracy of clustering methods since a bad clustering of clients causes a bad model performance in FL.

Results and Analysis: The results compared with baselines are listed in Table I. Note that we take five local training epochs and calculate the average accuracy of the last 20 rounds. Among all algorithms, our method achieves almost all the best outcomes. Some methods performs almost as well as CFLGT in several situations, because they get the right pre-defined number of clusters, which is impractical in real task (like scenario 3). With a wrong pre-defined cluster number, their performance decrease sharply while our method will not be influenced, which will be displayed in following part. In summary, The results echo the values of gradient trajectory about the model update and dataset distribution, which are

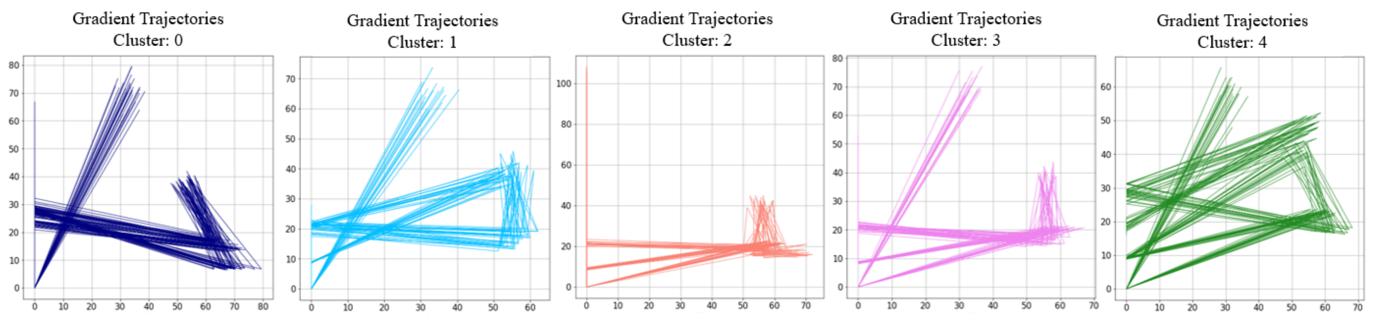

Fig. 6. Trajectories for clusters in scenario 1 based on Cifar10. Each one plots the trajectories of clients in one cluster, the output of clustering algorithm. It is clear that clients in the same cluster have similar trajectories. Some clusters of trajectories may have similar shape but have different coordinate values.(e.g. cluster 0 and cluster 1) These images prove that the clustering of trajectories in CFLGT is reasonable.

utilized in client clustering.

To evaluate the clustering of CFLGT, we visualize the trajectories of clusters in the experiment (scenario 1 based on Cifar10) as shown in Figure 6. Note that we set 5 dataset distributions among clients in scenario 1, and our method produces five groups of clients, which totally matches our setting. It shows that our method works correctly. Meanwhile, from Figure 6 we can see that there is apparent diversity between trajectories of clusters. Because a trajectory represents a client in the FL system, the diversity displays that our method indeed groups clients well. Additionally, we can see that clients in the same cluster have similar shapes of trajectories. It means that similar clients are clustered into the same group.

B. *No Need of Pre-defined Number of Cluster*

In the real-world task, it is hard for server to get information about clients' data distribution, resulting in a wrong pre-defined number of cluster. But our method relies itself to define the number of cluster, avoiding potential damage by wrong number of clusters. In this part, our experiments show the negative impact from wrong number of clusters on the FL system and the benefits of our method. Considering the high performance in the previous experiments, we choose FL+HC to testify to the damage from wrong cluster number for a better comparison. First, we add two extra baselines, FL+HC(10) and FL+HC(30). The first one represents 10 clusters as the input of FL+HC and another one represents 30 clusters as the input. The experiments are implemented in the scenario 3 based on Cifar10 (we set 20 distributions across clients). As a result, we compare our method with three baselines including: FL+HC(20) (right number of cluster), FL+HC(10) and FL+HC(30).

The results are shown in Table II, from which we can see that CFLGT can achieve good performance in scenario 3 as it does not need anything about dataset information. However, FL+HC algorithm with right number is almost as good as CFLGT. But FL+HC(10) and FL+HC(30) leads to reduced performance. The source of the problem is obvious. As shown in Figure 7, FL+HC(10) has fewer clusters than FL+HC(20), so the server arranges unique clients with other dissimilar clients into the same group, hurting the model aggregation in the group. FL+HC(30) has more clusters, so the server splits similar clients to different groups, hurting the model aggregation as well. Because in several groups, there is only one client, resulting in the aggregation as a failure.

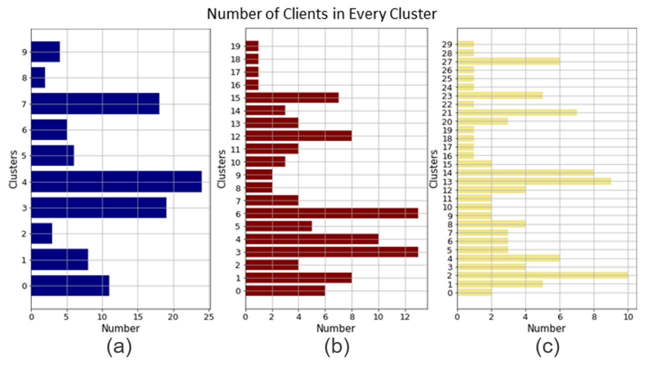

Fig. 7. Number of clients in each cluster for three baselines. The Y-axis represents the generated clusters and the X-axis shows the number of clients in each corresponding cluster. The results (a)(b)(c) are from FL+HC(10), FL+HC(20), and FL+HC(30) respectively.

TABLE II
PERFORMANCE COMPARISONS WITH OTHER BASELINES ON SCENARIO 3. THE FL+HC HAS THE CORRECT NUMBER OF CLUSTERS AS INPUT. THE AVERAGE ACCURACY OF THE LAST 20 ROUNDS ARE REPORTED AND THE FIGURE REPRESENTS THE PRE-DEFIEND NUMBER OF CLUSTER.

	FL+HC(10)	FL+HC(20)	FL+HC(30)	CFLGT
scenario3	67.90%	72.70%	70.51%	**73.49%**

C. *Efficiency Comparison*

We analyze the time cost and volume of uploaded data of CFL methods among the baselines. In the experiment, we set up a scenario closer to a complex environment in the real world, where the trained model is AlexNet [43] without batch norm layers and dropout layers. Every client's dataset contains 1500 images and all clients are involved during client clustering. We compare our method (CFLGT) with the CFL methods above (FL+HC, FedSem, and IFCA). Note that we set the number of clusters as 15 since there are 15 data distributions among clients. In the experiment, we focus on the consumption of computing resources and the needed bandwidth of these methods.

Consumption of computing resources: For the consumption of computing resources, the time-cost of CFLGT is the best. Since the clustering is composed of computation in client and

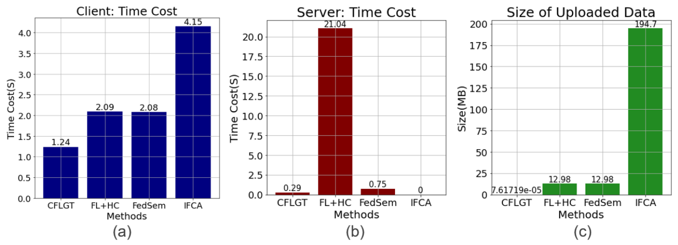

Fig. 8. Efficiency Comparison. The result (a) represents the time cost on client. The result (b) represents the time cost on server and the result (c) represents the size of uploaded data from client to server.

server, we analyze the time-cost on the client and the server separately. For time-cost on the client-side, Left plots in Figure 8 show that our method uses the least computing resources. The FL+HC and FedSem need to update the model, including complex back propagation. The IFCA requires every client to test all 15 global models on their dataset, causing huge consumption of computing resources. For the time-cost on the server site, the middle plot of Figure 8 shows that our method does not require the server to complete extensive calculations while the server in FL+HC is burdened with heavy work.

Bandwidth: We evaluate the required bandwidth by estimating the size of the uploaded data from the client. The results in Figure 8 (c) clarify that only a very low bandwidth is required in our method even though every client is involved in client clustering. The client just uploads its gradient trajectories, i.e., 0.078KB estimated in the experiment. In contrast, the other CFL methods need to upload the whole model parameters, which increases burden of communication when an huge model is implemented in the FL system. For example, BERT [44], an popular NLP model, contains over 300 million parameters sizing in 340 MB. If BERT is chosen as the training model, IFCA even needs server to broadcast BERT models of all clusters to every client.

The above results in consumption of resources and bandwidth show that our method can be used in a poor communication environment and a resource-constrained devices, and thus can be more practical in real-world tasks.

D. Privacy Protection

We set up a comparison experiment to testify to the privacy protection of CFLGT. Note that we only discuss the privacy protection about information exchange between clients and server and the rest of FL privacy issues are not included. Suppose there is an attacker disguised as a client in the FL system. The FL system is vulnerable to inference attacks, as every client contains one image as a dataset and updates only one time in local training in each round. If the attacker captures the update uploaded to the server by one of the clients, it can restore the raw image by the method in [22]. Specifically, the attacker generates a noisy image of the same size as the raw image, called fake image. Then it shortens the distance between the captured gradient and the gradient from the fake image in multiple iterations. The attacker utilizes the gradient descent method to update its fake image during the iterations until the distance is close to zero. Finally, the attacker can obtain an image very close to the raw image. Top right images in Figure 9 show a successful inference attack by the captured gradient of the whole model.

For CFLGT, we set up the worst-case situation, where the attacker obtains the pulling force and pushing force and then combines them into the gradient of the bottom layer. As a result, the attack can utilize the same inference method with the captured gradient of the bottom layer to restore raw data. However, the bottom right images in Figure 9 show that the attacker fails to obtain the raw image from the fake image since it still gets an image composed of noise after 300 iterations. Meanwhile, the left chart in Figure 9 exhibits that the gradient distance in the scenario remains much higher than the attack based on the gradient of the whole model. It means that the attacker cannot complete inference attack only with the gradient of the bottom layer in a model.

Note that in a real scenario of CFLGT, the attacker cannot even restore the pulling force and pushing force because it only captures the average values of pulling force and pushing force. Thus it is much harder to compute the gradient of the bottom layer. Therefore, our method, where clients only upload average values of pulling force and pushing force, is more robust on inference attacks.

VI. Conclusions and Future Work

In this paper we utilize the gradient of the bottom layer of model in Federated Learning and transform it into gradient trajectory. We show that with the trajectories from all the clients, the server can effectively observe the heterogeneity of the data. Based on this, we proposed a Clustered Federated Learning methods (CFLGT) where the server utilizes the gradient trajectory to cluster clients into groups and then aggregates models in every group. We have shown our method to be beneficial in theory and comprehensive experiments demonstrate its advantages in real world scenarios.

For future research, we plan to improve the client clustering mechanisms of the CFLGT so that it can perform accurate clustering when new clients join or clients' data changes. Plus, we also hope to expand our research to regression task and unsupervised task.

Acknowledgement

This work is supported with National Nature Science Foundation of China, No. 62072485, and Guangdong Basic and Applied Basic Research Foundation No. 2022A1515011294.

References

[1] A. Mehmood, I. Natgunanathan, Y. Xiang, G. Hua, and S. Guo, "Protection of big data privacy," *IEEE access*, vol. 4, pp. 1821–1834, 2016.
[2] B. McMahan, E. Moore, D. Ramage, S. Hampson, and B. A. y Arcas, "Communication-efficient learning of deep networks from decentralized data," in *Artificial intelligence and statistics*. PMLR, 2017, pp. 1273–1282.
[3] P. Kairouz, H. B. McMahan, B. Avent, A. Bellet, M. Bennis, A. N. Bhagoji, K. Bonawitz, Z. Charles, G. Cormode, R. Cummings *et al.*, "Advances and open problems in federated learning," *arXiv preprint arXiv:1912.04977*, 2019.
[4] Q. Li, Y. Diao, Q. Chen, and B. He, "Federated learning on non-iid data silos: An experimental study," 2021.

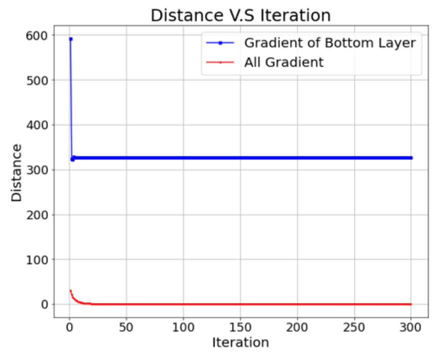

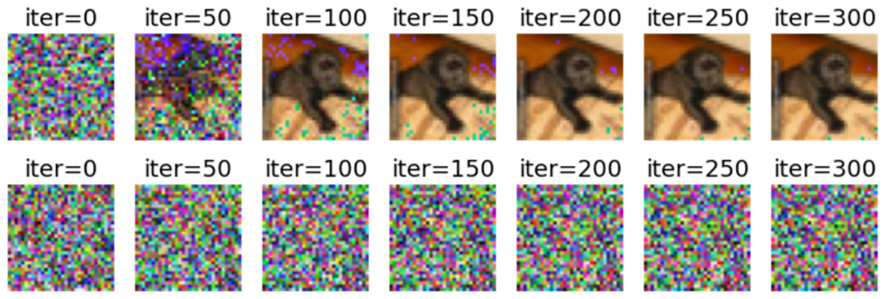

Fig. 9. Results in Gradient Leakage. The two sets of images on the right displays the update of fake image to original image as iteration grows. The upper one is based on gradient of whole model and another one is based on gradient of bottom layer of model. The figure on the left shows the change of gradient distance as the iteration increases.

[5] A. Nilsson, S. Smith, G. Ulm, E. Gustavsson, and M. Jirstrand, "A performance evaluation of federated learning algorithms," in *Proceedings of the second workshop on distributed infrastructures for deep learning*, 2018, pp. 1–8.

[6] X. Li, K. Huang, W. Yang, S. Wang, and Z. Zhang, "On the convergence of fedavg on non-iid data," *arXiv preprint arXiv:1907.02189*, 2019.

[7] M. Al-Shedivat, L. Li, E. Xing, and A. Talwalkar, "On data efficiency of meta-learning," in *International Conference on Artificial Intelligence and Statistics*. PMLR, 2021, pp. 1369–1377.

[8] A. Fallah, A. Mokhtari, and A. Ozdaglar, "Personalized federated learning with theoretical guarantees: A model-agnostic meta-learning approach," *Advances in Neural Information Processing Systems*, vol. 33, pp. 3557–3568, 2020.

[9] Z. Charles and J. Konečnỳ, "Convergence and accuracy trade-offs in federated learning and meta-learning," in *International Conference on Artificial Intelligence and Statistics*. PMLR, 2021, pp. 2575–2583.

[10] Y. Mansour, M. Mohri, J. Ro, and A. T. Suresh, "Three approaches for personalization with applications to federated learning," *arXiv preprint arXiv:2002.10619*, 2020.

[11] T. Li, S. Hu, A. Beirami, and V. Smith, "Ditto: Fair and robust federated learning through personalization," in *International Conference on Machine Learning*. PMLR, 2021, pp. 6357–6368.

[12] B. Sun, H. Huo, Y. Yang, and B. Bai, "Partialfed: Cross-domain personalized federated learning via partial initialization," *Advances in Neural Information Processing Systems*, vol. 34, 2021.

[13] V. Kulkarni, M. Kulkarni, and A. Pant, "Survey of personalization techniques for federated learning," in *2020 Fourth World Conference on Smart Trends in Systems, Security and Sustainability (WorldS4)*. IEEE, 2020, pp. 794–797.

[14] M. Luo, F. Chen, D. Hu, Y. Zhang, J. Liang, and J. Feng, "No fear of heterogeneity: Classifier calibration for federated learning with non-iid data," *arXiv preprint arXiv:2106.05001*, 2021.

[15] X.-C. Li and D.-C. Zhan, "Fedrs: Federated learning with restricted softmax for label distribution non-iid data," in *Proceedings of the 27th ACM SIGKDD Conference on Knowledge Discovery & Data Mining*, 2021, pp. 995–1005.

[16] L. Collins, H. Hassani, A. Mokhtari, and S. Shakkottai, "Exploiting shared representations for personalized federated learning," *arXiv preprint arXiv:2102.07078*, 2021.

[17] T. Li, A. K. Sahu, A. Talwalkar, and V. Smith, "Federated learning: Challenges, methods, and future directions," *IEEE Signal Processing Magazine*, vol. 37, no. 3, pp. 50–60, 2020.

[18] J. Yosinski, J. Clune, Y. Bengio, and H. Lipson, "How transferable are features in deep neural networks?" *arXiv preprint arXiv:1411.1792*, 2014.

[19] F. Sattler, K.-R. Müller, and W. Samek, "Clustered federated learning: Model-agnostic distributed multitask optimization under privacy constraints," *IEEE transactions on neural networks and learning systems*, 2020.

[20] M. Duan, D. Liu, X. Ji, R. Liu, L. Liang, X. Chen, and Y. Tan, "Fedgroup: Efficient federated learning via decomposed similarity-based clustering," in *2021 IEEE Intl Conf on Parallel & Distributed Processing with Applications, Big Data & Cloud Computing, Sustainable Computing & Communications, Social Computing & Networking (ISPA/BDCloud/SocialCom/SustainCom)*. IEEE, 2021, pp. 228–237.

[21] C. Briggs, Z. Fan, and P. Andras, "Federated learning with hierarchical clustering of local updates to improve training on non-iid data," in *2020 International Joint Conference on Neural Networks (IJCNN)*. IEEE, 2020, pp. 1–9.

[22] L. Zhu and S. Han, "Deep leakage from gradients," in *Federated learning*. Springer, 2020, pp. 17–31.

[23] L. Melis, C. Song, E. De Cristofaro, and V. Shmatikov, "Exploiting unintended feature leakage in collaborative learning," in *2019 IEEE Symposium on Security and Privacy (SP)*. IEEE, 2019, pp. 691–706.

[24] A. Ghosh, J. Chung, D. Yin, and K. Ramchandran, "An efficient framework for clustered federated learning," *arXiv preprint arXiv:2006.04088*, 2020.

[25] N. Gholizadeh and P. Musilek, "Federated learning with hyperparameter-based clustering for electrical load forecasting," *Internet of Things*, vol. 17, p. 100470, 2022.

[26] Y. Movshovitz-Attias, A. Toshev, T. K. Leung, S. Ioffe, and S. Singh, "No fuss distance metric learning using proxies," in *Proceedings of the IEEE International Conference on Computer Vision*, 2017, pp. 360–368.

[27] J. Snell, K. Swersky, and R. S. Zemel, "Prototypical networks for few-shot learning," *arXiv preprint arXiv:1703.05175*, 2017.

[28] A. Zhai and H.-Y. Wu, "Making classification competitive for deep metric learning," *arXiv preprint arXiv:1811.12649*, vol. 11, 2018.

[29] A. Wainakh, F. Ventola, T. Müßig, J. Keim, C. G. Cordero, E. Zimmer, T. Grube, K. Kersting, and M. Mühlhäuser, "User label leakage from gradients in federated learning," *arXiv preprint arXiv:2105.09369*, 2021.

[30] J. Geiping, H. Bauermeister, H. Dröge, and M. Moeller, "Inverting gradients–how easy is it to break privacy in federated learning?" *arXiv preprint arXiv:2003.14053*, 2020.

[31] B. Zhao, K. R. Mopuri, and H. Bilen, "idlg: Improved deep leakage from gradients," *arXiv preprint arXiv:2001.02610*, 2020.

[32] C. E. Brown, "Coefficient of variation," in *Applied multivariate statistics in geohydrology and related sciences*. Springer, 1998, pp. 155–157.

[33] X. Li, M. Jiang, X. Zhang, M. Kamp, and Q. Dou, "Fedbn: Federated learning on non-iid features via local batch normalization," *arXiv preprint arXiv:2102.07623*, 2021.

[34] A. Katharopoulos and F. Fleuret, "Not all samples are created equal: Deep learning with importance sampling," in *International conference on machine learning*. PMLR, 2018, pp. 2525–2534.

[35] Y. He, J. Ren, G. Yu, and J. Yuan, "Importance-aware data selection and resource allocation in federated edge learning system," *IEEE Transactions on Vehicular Technology*, vol. 69, no. 11, pp. 13 593–13 605, 2020.

[36] D. Dueck, *Affinity propagation: clustering data by passing messages*. Citeseer, 2009.

[37] A. Banerjee and R. N. Dave, "Validating clusters using the hopkins statistic," in *2004 IEEE International conference on fuzzy systems (IEEE Cat. No. 04CH37542)*, vol. 1. IEEE, 2004, pp. 149–153.

[38] V. Mothukuri, R. M. Parizi, S. Pouriyeh, Y. Huang, A. Dehghantanha, and G. Srivastava, "A survey on security and privacy of federated learning," *Future Generation Computer Systems*, vol. 115, pp. 619–640, 2021.

[39] B. Hitaj, G. Ateniese, and F. Perez-Cruz, "Deep models under the gan: information leakage from collaborative deep learning," in *Proceedings of the 2017 ACM SIGSAC Conference on Computer and Communications Security*, 2017, pp. 603–618.

[40] D. Li and J. Wang, "Fedmd: Heterogenous federated learning via model distillation," *arXiv preprint arXiv:1910.03581*, 2019.

[41] F. Yu, A. S. Rawat, A. Menon, and S. Kumar, "Federated learning with only positive labels," in *International Conference on Machine Learning*. PMLR, 2020, pp. 10 946–10 956.

[42] F. Murtagh and P. Contreras, "Algorithms for hierarchical clustering: an overview," *Wiley Interdisciplinary Reviews: Data Mining and Knowledge Discovery*, vol. 2, no. 1, pp. 86–97, 2012.

[43] A. Krizhevsky, I. Sutskever, and G. E. Hinton, "Imagenet classification with deep convolutional neural networks," *Advances in neural information processing systems*, vol. 25, 2012.

[44] I. Tenney, D. Das, and E. Pavlick, "Bert rediscovers the classical nlp pipeline," *arXiv preprint arXiv:1905.05950*, 2019.

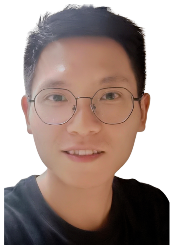

Ruiqi Liu Received the bachelor's degree in Engineering from Sun Yat-Sen University. He is currently pursuing the master's degree at Georgia Institute of Technology.

Junbo Wang received his B.S. and M.S. degrees in Electrical and Electronic Engineering from Yanshan University, China and his Ph.D. degree in Computer Science and Engineering from the University of Aizu, Japan in 2011. He was a Postdoctoral Scholar and Associate Professor in the Univeristy of Aizu, Japan. Current he is an Associate Professor in School of Intelligent Systems Engineering, Sun Yat-sen University, China. He was the PI at Japan site for JST-NSF Joint Funding Program to study Big Data and Disaster (SICORP Project). Currently his research interests include collaborative ML, federated learning, fog computing, big data and privacy.

Songcan Yu received his B.S. degree in automation and M.S. degree in pattern recognition and intelligent systems from School of Electronic Information Engineering, Inner Mongolia University in 2015 and 2020, respectively. He is pursuing his Ph.D. degree at School of Intelligent Systems Engineering, Sun Yat-sen University, China. His research interests include federated learning, pattern recognition.

Krishna Kant is currently a professor in the Computer and Information Science Department at Temple University in Philadelphia, PA, where he directs the IUCRC center on Intelligent Storage. Earlier he was a research professor in the Center for Secure Information Systems at George Mason University. From 2008-2013 he served as a program director at NSF where he managed the computer systems research program and was instrumental in the development and running of NSF-wide sustainability initiative named science, engineering and education for sustainability (SEES). Prior to NSF, he served in industry for 18 years (at Intel, Bellcore, and Bell Labs) and 10 years in academia (at Penn State and Northwestern Univ.). He carries a combined 41 years of experience in academia, industry, and government. His research interests span a wide range including data center storage and networking, communications in challenging environments, and robustness and security in cyber and cyber-physical systems. He is a Fellow of the IEEE.